

# Tau associated peripheral and central neurodegeneration: Identification of an early imaging marker for tauopathy

Alexandra Marquez<sup>a</sup>, Lucie S. Guernsey<sup>a</sup>, Katie E. Frizzi<sup>a</sup>, Morgan Cundiff<sup>a</sup>, Isabel Constantino<sup>a</sup>, Nabeel Muttalib<sup>a</sup>, Fernanda Arenas<sup>a</sup>, Xiajun Zhou<sup>a</sup>, Sze Hway Lim<sup>b</sup>, Maryam Ferdousi<sup>d</sup>, Georgios Ponirakis<sup>e</sup>, Monty Silverdale<sup>b,c</sup>, Christopher Kobylecki<sup>b,c</sup>, Matthew Jones<sup>b</sup>, Andrew Marshall<sup>f</sup>, Rayaz A. Malik<sup>g</sup>, Corinne G. Jolival<sup>a,\*</sup>

<sup>a</sup> Department of Pathology, University of California San Diego, USA

<sup>b</sup> Department of Neurology, Manchester Centre for Clinical Neurosciences, Salford Royal NHS Foundation Trust, Salford, UK

<sup>c</sup> Manchester Academic Health Sciences Centre, University of Manchester, UK

<sup>d</sup> Institute of Cardiovascular Sciences, University of Manchester and Central Manchester NHS Foundation Trust, Manchester Academic Health Science Centre, Manchester, UK

<sup>e</sup> Weill Cornell Medicine-Qatar, Doha, Qatar

<sup>f</sup> Department of Clinical Neurophysiology, Salford Royal Hospital, National Health Service Foundation Trust, Institute of Brain, Behaviour and Mental Health, University of Manchester, Manchester, UK

<sup>g</sup> Department of Medicine, Weill Cornell Medicine-Qatar, Doha, Qatar and Institute of Cardiovascular Science, University of Manchester, Manchester, UK

## ARTICLE INFO

### Keywords:

Corneal confocal microscopy  
Memory deficits  
Neurodegeneration  
Peripheral neuropathy  
Tau

## ABSTRACT

Pathological hyperphosphorylated tau is a key feature of Alzheimer's disease (AD) and Frontotemporal dementia (FTD). Using transgenic mice overexpressing human non-mutated tau (htau mice), we assessed the contribution of tau to peripheral and central neurodegeneration. Indices of peripheral small and large fiber neuropathy and learning and memory performances were assessed at 3 and 6 months of age. Overexpression of human tau is associated with peripheral neuropathy at 6 months of age. Our study also provides evidence that non-mutated tau hyperphosphorylation plays a critical role in memory deficits. In addition, htau mice had reduced stromal corneal nerve length with preservation of sub-basal corneal nerves, consistent with a somatofugal degeneration. Corneal nerve degeneration occurred prior to any cognitive deficits and peripheral neuropathy. Stromal corneal nerve loss was observed in patients with FTD but not AD. Corneal confocal microscopy may be used to identify early neurodegeneration and differentiate FTD from AD.

## 1. Introduction

Tau is a microtubule-associated protein that plays a role in microtubule assembly and stability (Weingarten et al., 1975), cell morphogenesis, cell division and intracellular trafficking (Takashima et al., 2019). Tau is also involved in neuronal signaling and synaptic plasticity (Hanger et al., 2019). A number of post-translational alterations modify tau proteins by phosphorylation and formation of filamentous inclusions (Goedert et al., 2017). Some of these post-translational modifications lead to pathological tau aggregates that are associated with neurodegeneration in transgenic rodents (Goedert et al., 2017) and in patients with Alzheimer's disease (AD) (Lowe et al., 2018). Seminal work on frontotemporal dementia (FTD), particularly frontotemporal dementia

associated with Parkinsonism (FTDP-17T or FTLD-tau) demonstrated that pathological formation of assembled tau can cause neurodegeneration and dementia (Hutton et al., 1998; Poorkaj et al., 1998; Spillantini et al., 1996). FTD is the second leading cause of dementia in people younger than 65 years old and is a heterogeneous group of familial and sporadic neurodegenerative disorders encompassing several clinical sub-groups. The FTLD-tau sub-group and AD are part of the clinically heterogeneous neurodegenerative disorders collectively termed tauopathies, as they are pathologically defined by tau-positive deposits in the brain (Orr et al., 2017). PET imaging studies have shown that cognition correlates better with tau pathology than with Aβ plaque deposition (Brier et al., 2016; Johnson et al., 2016), suggesting that tau pathology likely contributes to cognitive decline in AD,

\* Corresponding author at: 9500 Gilman Drive, La Jolla, CA 92093-0612, E-mail address: [cjolival@ucsd.edu](mailto:cjolival@ucsd.edu) (C.G. Jolival).

<https://doi.org/10.1016/j.nbd.2021.105273>

Received 4 January 2021; Accepted 15 January 2021

Available online 19 January 2021

0969-9961/© 2021 The Authors.

Published by Elsevier Inc.

This is an open access article under the CC BY-NC-ND license

(<http://creativecommons.org/licenses/by-nc-nd/4.0/>).

supporting a causative role of tau in neurodegeneration and dementia.

A number of mouse models of tauopathy/FTD are available that reflect many of the pathogenic alterations found in clinical studies (Ahmed et al., 2017; Roberson, 2012). Mouse models of tauopathy/FTD induced by genetic mutations represent FTD patients with a family history of dementia. However, the majority of tauopathy/FTD cases are not associated with tau mutations. To model the sporadic tauopathy/FTD population, we used transgenic mice expressing human non-mutant tau (6 isoforms) at levels 3.7-fold greater than murine tau, the human tau mouse (htau) (Andorfer et al., 2003). In this model, hyperphosphorylated tau can be detected in cell bodies and dendrites by 3 months of age (Andorfer et al., 2003) and slower visuospatial learning is detected by 6 months of age (Phillips et al., 2011). To-date, studies assessing the expression of tau and its functional and structural consequences in peripheral nerves are limited to rodents (Tolkovsky and Brelstaff, 2018; Vacchi et al., 2020; Yi et al., 2019). Peripheral nerve functions can easily be assessed in-vivo and our studies have utilized corneal confocal microscopy (CCM) to identify neurodegeneration in a range of peripheral and central neurodegenerative diseases, including PD (Kass-Iliyya et al., 2015; Podgorny et al., 2016a) and dementia (Al-Janahi et al., 2020; Ponirakis et al., 2019). We have assessed cognitive functions, multiple indices of peripheral nerve dysfunction/degeneration and corneal nerve degeneration in htau mice and undertaken CCM in patients with FTD and AD.

## 2. Materials and methods

### 2.1. Animals

Female human tau mice (htau,  $N = 7$ ) were purchased from Jackson lab (stock #: 005491B6.Cg-Mapt<tm1(EGFP)Klt>Tg(MAPT)8cPdav/J). All six isoforms (including both 3R and 4R forms) of human MAPT are expressed. Hyperphosphorylated MAPT is detected in cell bodies and dendrites by three months of age. Female C57Bl6/J mice ( $N = 10$ ) were used as controls (stock # 000664). Groups of 7 to 10 mice were housed 4–5 per cage with free access to water and food (5001 PMI diet, Harlan, Indianapolis, USA). Studies followed protocols approved by the Institutional Animal Care and Use Committee of the University of California, San Diego.

### 2.2. Models of Alzheimer's disease

The transgenic hAPP mice (Rockenstein et al., 2003; Rockenstein et al., 2001; Rockenstein et al., 2007) and the TAPP transgenic mice were used as models of AD. The hAPP transgenic mice express mutated (London V717I and Swedish K670M/N671L) hAPP751 under the control of the neuronal murine (m)Thy-1 promoter (Rockenstein et al., 2001). Transgenic lines were maintained by crossing heterozygous transgenic mice with non-transgenic wild type (WT) C57BL/6 x DBA/2 F1 breeders. All mice ( $N = 5$ ) were female and heterozygous with respect to the transgene. Wild type female littermates ( $N = 8$ ) were used as controls. A second model of AD was used: double transgenic mice expressing both amyloid precursor protein (APP) and tau (Tg(APPsWE)2576KhaTg(Prnp-MAPT\*P301L)JNPL3Hlmc, abbreviated as TAPP) and wild type (mixed background C57Bl6, SJL, DBA/2, SW) mice from Taconic, USA. These TAPP mice carry the transgene coding for the 695-amino acid isoform of human  $\beta$ -amyloid (A $\beta$ ) protein in addition to the transgene for the human P301L mutation of MAPT. Double transgenic mice (mutant human APP and human tau: TAPP) develop a few plaques and neurofibrillary tangles (NFT) in the limbic system by 6 months of age that become numerous by 8–9 months of age (Lewis et al., 2001). The TAPP transgenic ( $N = 8$ ) and Wild type ( $N = 10$ ) mice were female and part of a study recently published (King et al., 2020).

### 2.3. Learning test

Learning ability was assessed using the Barnes maze test as described previously (Jolivald et al., 2010; Jolivald et al., 2008). Briefly, the Barnes circular maze consists of an illuminated white circular platform (92 cm diameter) with 20 holes (5 cm diameter) equally spaced and located 5 cm from the perimeter. A black escape box was placed under one of the holes for the learning phase of the test. A cue (red arrow) was placed behind the hole with the escape box. The mouse was placed in the middle of the platform and allowed to explore the maze. Timing of the session ended when the mouse found the box or after 5 min had elapsed. The time to find the box was recorded. Mice were tested at 3–4 and 6 months of age, once a day, for 5 consecutive days.

### 2.4. Memory tests

The object recognition test was performed to assess episodic short-term (1 h) memory without an acquisition phase. After a 1 min habituation in the empty chamber, the mouse was exposed to 2 similar objects until a combined time spent on the 2 objects reached 20s. If the 20s observation was not reached within 8 min, the mouse was not included further in the test. After 1 h back in its home cage, the mouse was exposed to 1 of the previous objects and 1 novel object. The mouse was given 5 min to explore both objects. The amount of time taken to explore the new object ( $t_2$ ), relative to the time spent on the first object ( $t_1$ ), provides a memory index where % recognition index =  $((t_2 - t_1)/(t_1 + t_2)) \times 100$  (Ennaceur and Delacour, 1988). A lack of recognition of the novel object results in a negative recognition index. Long-term memory was assessed using the Barnes maze (Jolivald et al., 2008). Mice were placed on the Barnes maze and allowed to locate the escape box on 5 consecutive days to facilitate learning (acquisition phase, see above). The test was repeated 3 days later to assess memory of the learned behavior (retention phase). Mice were tested at 3–4 and 6 months of age.

### 2.5. Tactile responses

Paw responsiveness to light touch (stimulation to large A $\beta$  fibers) was measured using Von Frey filaments (Jolivald et al., 2016) at 3–4 and 6 months of age. Both hind paws were tested, and the mean used to represent the 50% paw withdrawal threshold (50% PWT).

### 2.6. Thermal responses

Paw withdrawal from heat (stimulation of small C fibers) was measured using a thermal testing apparatus (UARD, San Diego, USA) with the glass surface maintained at 30 °C at 3–4 and 6 months of age. Both hind paws were tested 3 times at 5 min intervals, the median response time for each paw calculated and the mean of the two medians used to represent each mouse (Jolivald et al., 2016).

### 2.7. Electrophysiology

Motor nerve conduction velocity (MNCV) of large fibers was measured in the sciatic nerve:interosseus muscle system (stimulation at 200 mV, 50  $\mu$ s duration square wave stimulus every 2 s) of isoflurane-anesthetized animals (Jolivald et al., 2016) at 3–4 and 6 months of age. Three measurements were made per mouse and MNCV calculated using the median value and distance between the stimulation points.

### 2.8. Epidermal nerve visualization and quantification

Animals were killed at 6 months of age and the hind paw plantar skin removed into 4% paraformaldehyde for 24 h. Samples were embedded in paraffin and cut as 6  $\mu$ m sections before incubation with antibodies against the pan-neuronal marker PGP 9.5 (1:1000, Biogenesis Ltd., UK). Slides were coded and epidermal PGP9.5 immunoreactive profiles

quantified by light microscopy (Jolivald et al., 2016).

## 2.9. Corneal nerve imaging and quantification

Mice were anesthetized with isoflurane and placed in a custom-designed imaging platform connected to a Heidelberg Retina Tomograph 3 with Rostock corneal module (Heidelberg Engineering, Heidelberg, Germany). The image collecting procedure is described elsewhere (Jolivald et al., 2016). Nerve occupancy using Image J software was calculated in sequential images (2  $\mu$ m spacing) of the sub-basal and stroma plexus. The analysis of the first 10 images of the stroma is represented in Fig. 2E.

## 2.10. Tau immunostaining

At 6 months of age, mice were sacrificed by decapitation after brief isoflurane anesthesia in accordance with NIH guidelines for the humane treatment of animals. Caution was taken to remove the brain within a minute of decapitation to preserve phosphorylation status. Brains were removed and divided sagittally. One hemibrain was post-fixed in phosphate-buffered 4% paraformaldehyde (pH 7.4) at 4 °C for 48 h., dehydrated and processed into paraffin, then sectioned at 6  $\mu$ m with a Leitz 1512 Rotary Microtome (Leitz, Germany) while the other hemibrain was prepared for Western blot analysis. 6  $\mu$ m-thick paraffin sections were mounted onto Superfrost Plus slides (#12–550-15, Fisher Scientific, USA) and immunolabeled with mouse antibody against tau (#MAB361, Millipore, USA) and rabbit antibody against tau S199/202 phosphorylation (#AB9674, Covance, USA). Briefly, sections were incubated overnight at 4 °C with the tau (1:100) or tau phosphorylation (1:500) antibodies, followed by a 1 h secondary antibody incubation in 1:500 AlexaFluor 488 goat anti-mouse (#A11001, Invitrogen, USA) or goat anti-rabbit (#A11034, Invitrogen, USA), respectively. Sections were counterstained with 0.25  $\mu$ g/mL DAPI (#D1306, Molecular Probes, USA) for 10 min. Sections were analyzed by an observer who was unaware of the animal group using an Olympus BX51 microscope configured for fluorescence. Fluorescent images of the hippocampus were taken at 20 $\times$  magnification using the Live Tiling option in Image Pro Premier software (Media Cybernetics, USA). Using MATLAB software (MathWorks, USA), the pixels corresponding to non-immunoreactive structures (e.g. blood vessels or folded tissue) within the hippocampus and any areas outside of the hippocampus were removed. The remaining pixels corresponded to the immunoreactivity of the antibody of choice in the hippocampus and were quantified using MATLAB.

## 2.11. Western blotting

Hippocampi and sciatic nerves were homogenized in buffer (50 mM Tris-HCl pH 7.4, 150 mM NaCl, 0.5% Triton X, 1 mM EDTA, protease inhibitor cocktail). Fifty  $\mu$ l of the hippocampus homogenate were boiled for 5 min, iced for 5 min and then centrifuged to purify the preparation as tau proteins are heat resistant. Protein concentration was assessed using the bicinchoninic acid method (BCA protein assay kit, Pierce, Rockford, IL, USA). Boiled hippocampus homogenates (5  $\mu$ g) and sciatic nerve homogenates (20  $\mu$ g) were separated on 4–12% SDS-PAGE Bis-Tris gels (Novex, Invitrogen, Carlsbad, CA, USA) and immunoblotted onto nitrocellulose as described previously (Jolivald et al., 2008). Blots were incubated with antibodies against phosphorylated tau (T231, 1/3000, Chemicon, cat# AB9668), tau (1/3000, tau 5 clone, Chemicon, cat#-MAB361) or high molecular tau (HMW, 1/3000, generously provided by Dr. Itzhak Fisher, Drexel University) followed by the corresponding secondary antibodies tagged with infrared dyes (IRDye, 1/15000, LI-COR Biosciences, Lincoln, NE, USA). For each animal, band intensities were normalized by calculating the ratio of the intensity of the band corresponding to phosphorylated tau to total tau for hippocampi and sciatic nerves or phosphorylated HMW/HMW tau for the sciatic nerves. Two-3 blots were replicated at least 3 times and intensity values were

averaged to provide the percent intensities reported.

## 2.12. Plasma analysis

Plasma obtained at termination of the study (6 month of age) was assessed for insulin (Ultrasensitive mouse insulin ELISA, Mercodia AB, Uppsala, Sweden), and for triglycerides and cholesterol levels using the oxygen-rate analyzer GM7 (Analox Instruments, Lunenburg, MA, USA).

## 2.13. Patients

### 2.13.1. FTD patients

Two patients with FTD were recruited from the Cerebral Function Unit, Greater Manchester Neuroscience Centre, Salford Royal Foundation Trust (UK). They presented with progressive behavioral change (apathy, reduced empathy, routine bound/obsessive, sweet food fads, obsessions, executive dysfunction) and abnormalities on SPECT and MRI imaging. Both patients fulfilled clinical and imaging criteria for probable FTD.

### 2.13.2. AD patients

Three patients with AD (ICD-10 criteria) were recruited from the Geriatric and Memory clinic in Rumailah Hospital, Doha, Qatar. Patients with severe anxiety, severe depression, Parkinson's disease, fronto-temporal dementia and Lewy body dementia, hypomania, and severe dementia who were unable to cooperate were excluded. Additionally, patients with other potential causes of peripheral neuropathy including vitamin B<sub>12</sub> deficiency, hypothyroidism, HIV infection and hepatitis C were excluded. Patients with dry eyes, corneal dystrophies, ocular trauma or surgery in the preceding 6 months were excluded. This study was approved by the Institutional Review Board of Weill Cornell Medicine in Qatar and Hamad Medical Corporation and all participants gave informed consent to take part in the study. The research adhered to the tenets of the declaration of Helsinki. Cognitive screening was performed using the Montreal Cognitive Assessment (MoCA) test. The MoCA assesses seven cognitive domains including visuospatial/executive, naming, memory, attention, language, abstraction and delayed recall giving a total score of 30. A score of  $\leq 26$  indicates cognitive impairment.

### 2.13.3. Corneal confocal microscopy

CCM was performed with the Heidelberg Retinal Tomograph III Rostock Cornea Module (Heidelberg Engineering GmbH, Heidelberg, Germany). The cornea was locally anesthetized by instilling 1 drop of 0.4% benoxinate hydrochloride (Chauvin Pharmaceuticals, Chefaro, UK) and Viscotears (Carbomer 980, 0.2%, Novartis, UK) was used as the coupling agent between the cornea and the TomoCap as well as between the TomoCap and the objective lens. Several scans of the stroma and sub-basal nerve plexus in the central cornea were captured per eye over ~5 min. Three high clarity images of the sub-basal plexus per eye were selected by one researcher based on depth, focus position and contrast (Kalteniece et al., 2017). Corneal nerve fiber length (CNFL) (total fiber length mm/mm<sup>2</sup>) was quantified using CCMetrics, a validated image analysis software (Dabbah et al., 2011). The 10 first images of the stroma were analyzed to quantify stromal nerve length in the same manner as images taken from mice.

## 2.14. Data analysis

All animals and tissues were coded during assay to prevent observer bias. Data are presented as group mean  $\pm$  SEM. Statistical comparisons were made using unpaired *t*-test between 2 groups.

**Table 1**Physiological and metabolic parameters at 6 months of age. \* $p < 0.05$  vs wild type (WT) group using unpaired  $t$ -test.

Group	N	Weight (g) Start	Weight (g) End	Glucose (mg/dl)	Insulin ( $\mu$ g/l)	Cholesterol (mmol/l)	Triglycerides (mmol/l)
WT	10	18.1 $\pm$ 0.2	22.0 $\pm$ 0.5	140.9 $\pm$ 6.1	0.71 $\pm$ 0.46	1.75 $\pm$ 0.10	1.13 $\pm$ 0.15
htau	7	18.4 $\pm$ 0.6	22.3 $\pm$ 0.4	155.6 $\pm$ 7.8	0.66 $\pm$ 0.07	1.77 $\pm$ 0.07	1.22 $\pm$ 0.10

### 3. Results

#### 3.1. Physiological and metabolic parameters

Htau mice had a similar body weight to WT mice at the start and the end of study (Table 1). Blood glucose, insulin, cholesterol and triglycerides levels remained similar to the levels in WT mice (Table 1).

#### 3.2. Tau phosphorylation in the hippocampus

Phosphorylated tau normalized to the level of total tau was significantly ( $p < 0.05$ ) increased in the hippocampus of htau mice (WT: 100.0  $\pm$  25.9, htau: 377.4  $\pm$  83.7% intensity). This was confirmed by Western blot analysis of phosphorylated tau (WT: 100.0  $\pm$  17.9, htau: 209.2  $\pm$  23.4\*\*\*% intensity).

#### 3.3. Memory impairment

At 4 months of age, htau mice did not display significant impairment in learning or retention in the Barnes maze test (Fig. 1A, B). At 6 months of age, learning ability of the htau mice was similar to WT mice (Fig. 1A), but long-term memory in the Barnes maze test was significantly ( $P < 0.05$ ) affected in htau mice (Fig. 1B).

Short-term episodic memory assessed with the ORT in htau mice was similar to WT mice at 4 months (Fig. 1C), but was significantly ( $P < 0.01$ ) impaired at 6 months of age (Fig. 1C).

#### 3.4. Peripheral neuropathy

At 4 months of age, MNCV and indices of tactile and thermal responses were normal in htau mice (Fig. 2A, B, C). At 6 months of age, htau mice developed significant MNCV slowing ( $P < 0.001$ ), paw tactile allodynia ( $P < 0.05$ ), paw heat hypoalgesia ( $P < 0.01$ ) accompanied by reduced paw IENF density ( $P < 0.01$ , Fig. 2A, B, C, D) compared with WT.

#### 3.5. Corneal stromal and sub-basal plexus nerves-mice

Stromal corneal nerve occupancy was significantly ( $p < 0.01$ ) reduced in htau at 4 months and 6 months (Fig. 2E, F) compared with WT mice. There was no reduction in corneal sub-basal nerve occupancy at 4 months (WT: 10.9  $\pm$  0.9, htau: 9.3  $\pm$  1.7%) and 6 months (WT: 8.2  $\pm$  0.6, htau: 8.2  $\pm$  0.8%) (Supplementary Fig. 1).

#### 3.6. Tau phosphorylation in the periphery

HMW tau was detected in the sciatic nerve of WT mice and to a significantly reduced level, with a slightly higher molecular weight, in htau mice (Fig. 2Gi and H). In contrast, the small isoforms of tau (50–60 kDa) were significantly ( $p < 0.05$ ) increased in htau mice compared with WT mice (Fig. 2Gii and H). Phosphorylated tau normalized to the level of total tau or HMW tau, respectively, was significantly increased in the sciatic nerve of htau mice for both the small (50–60 kDa) ( $p < 0.05$ ) and HMW tau ( $p < 0.001$ ) compared with WT mice (Fig. 2Giii and I).

#### 3.7. APP and TAPP mice

Similar behavior assays (Barnes and ORT) and corneal nerve

assessment were undertaken in 2 models of AD, the human amyloid precursor protein (APP) mice (Rockenstein et al., 2001; Jolivald et al., 2010) and the TAPP mice (Lewis et al., 2001; King et al., 2020). Both transgenic mice strains overexpress human APP but only TAPP mice also overexpress human tau protein. APP transgenic mice were maintained for 1 year with bimonthly CCM imaging and behavior assays. Despite the presence of learning impairment in the Barnes maze test at 1 year of age (Fig. 3B), there was no difference in memory (Fig. 3C) and in stromal nerve occupancy in APP mice compared with age-matched WT mice (Fig. 3A). Sub-basal nerve plexus occupancy did not differ between WT and APP mice (WT: 66.5  $\pm$  2.9, APP: 75.3  $\pm$  5.3% occupancy).

In contrast, TAPP mice had a significantly ( $p < 0.05$ ) decreased stromal nerve occupancy at 4 months of age ( $p < 0.05$ ) (Fig. 3D), with no change in sub-basal plexus nerve occupancy (WT: 49.8  $\pm$  2.7, TAPP: 52.4  $\pm$  3.8). Four months old TAPP mice showed significantly ( $P < 0.01$ ) impaired learning abilities in the acquisition phase but not the retention phase of the Barnes maze or the object recognition test (Fig. 3E, F).

#### 3.8. Corneal stromal and sub-basal plexus nerves-humans

The MOCA score in patients with AD was lower than in controls (Table 2).

Corneal nerve occupancy tended to be reduced in the stroma of FTD patients and increased in the stroma of AD patients (Table 2, Fig. 4). Similar results were obtained when combining dementia types (AD, Vascular dementia and mixed,  $N = 11$ , corneal nerve occupancy: 244.7  $\pm$  73.6 pixels). Sub-basal plexus corneal nerve fiber length did not differ in FTD patients (aged-matched control: 24.26  $\pm$  3.6 vs FTD: 21.35  $\pm$  1.9 mm/mm<sup>2</sup>) but was reduced in AD patients (aged-matched control: 26.4  $\pm$  5.1 vs AD: 12.7  $\pm$  7.6 mm/mm<sup>2</sup>).

### 4. Discussion

Our data demonstrate that the presence of human non-mutated tau is sufficient to cause peripheral neuropathy. Our study provides additional evidence that tau plays a critical role in memory deficits and is associated with an early reduction of stromal corneal nerves with a preserved sub-basal nerve plexus and could be used as an imaging biomarker for FTD.

Tau has been shown to play an important role in synaptic function in healthy neurons (Regan et al., 2017). Patients with behavioral variant FTD (bv-FTD) experience episodic memory deficits (Hornberger and Piguet, 2012) and the extent of memory impairment is comparable to that observed in AD patients (Hornberger et al., 2010; Irish et al., 2014; Pennington et al., 2011). There are also significant memory deficits in R406W mutated tau mice (Tatebayashi et al., 2002) and P301L transgenic mice (Ramsden et al., 2005) with an improvement of memory after suppression of transgenic tau in a conditional mouse with P301L tau overexpression (Santacruz et al., 2005). While Morris water maze spatial learning and memory remained unaffected in 15 months old htau mice (Trujillo-Estrada et al., 2019), htau mice have been shown to develop cognitive deficits in the object recognition memory task at 12 months of age (Polydoro et al., 2009). These deficits were not present at 4 months of age (Polydoro et al., 2009). In this study, we have shown that overexpressed human non-mutated hyperphosphorylated tau was sufficient to induce short-term episodic memory deficits by 6 months of age but with no effect on learning ability. Our previous studies showed that STZ-diabetes induced deficits in learning and memory after 8 weeks of

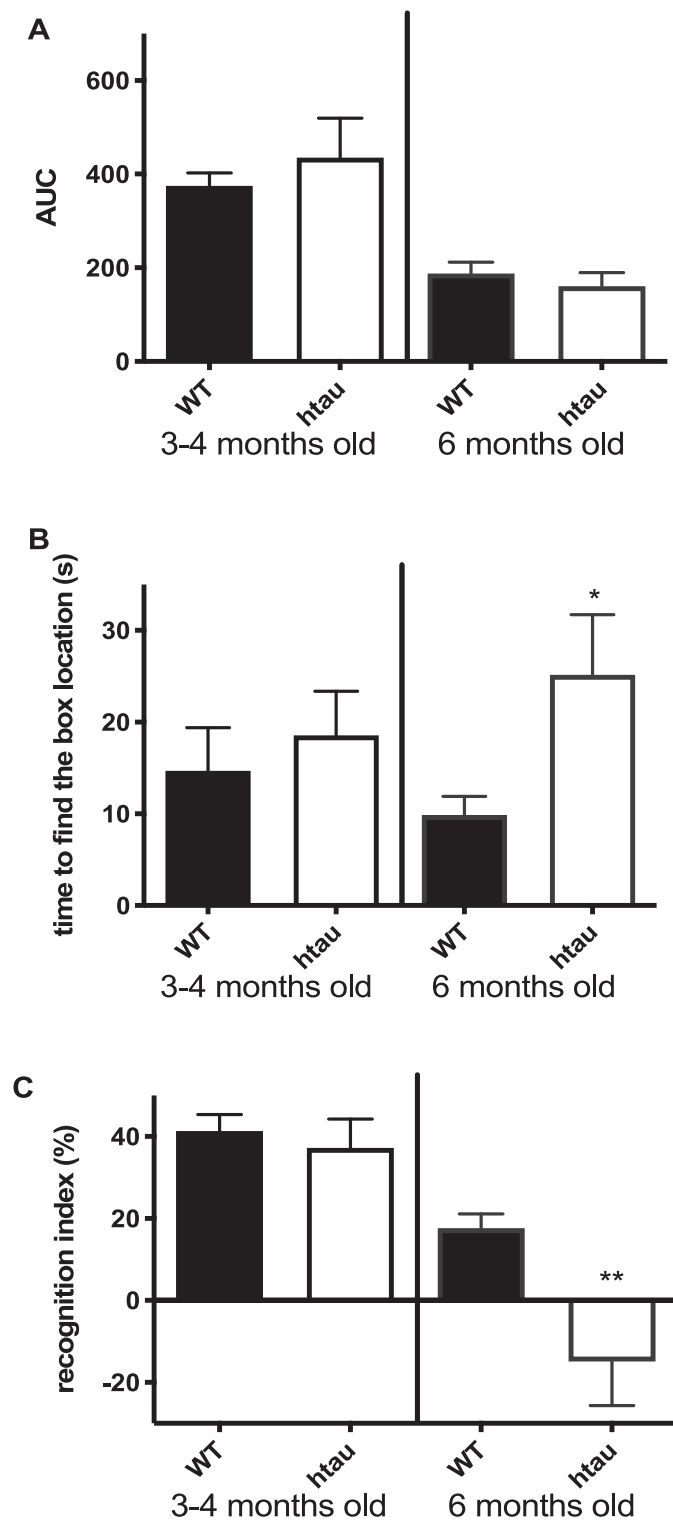


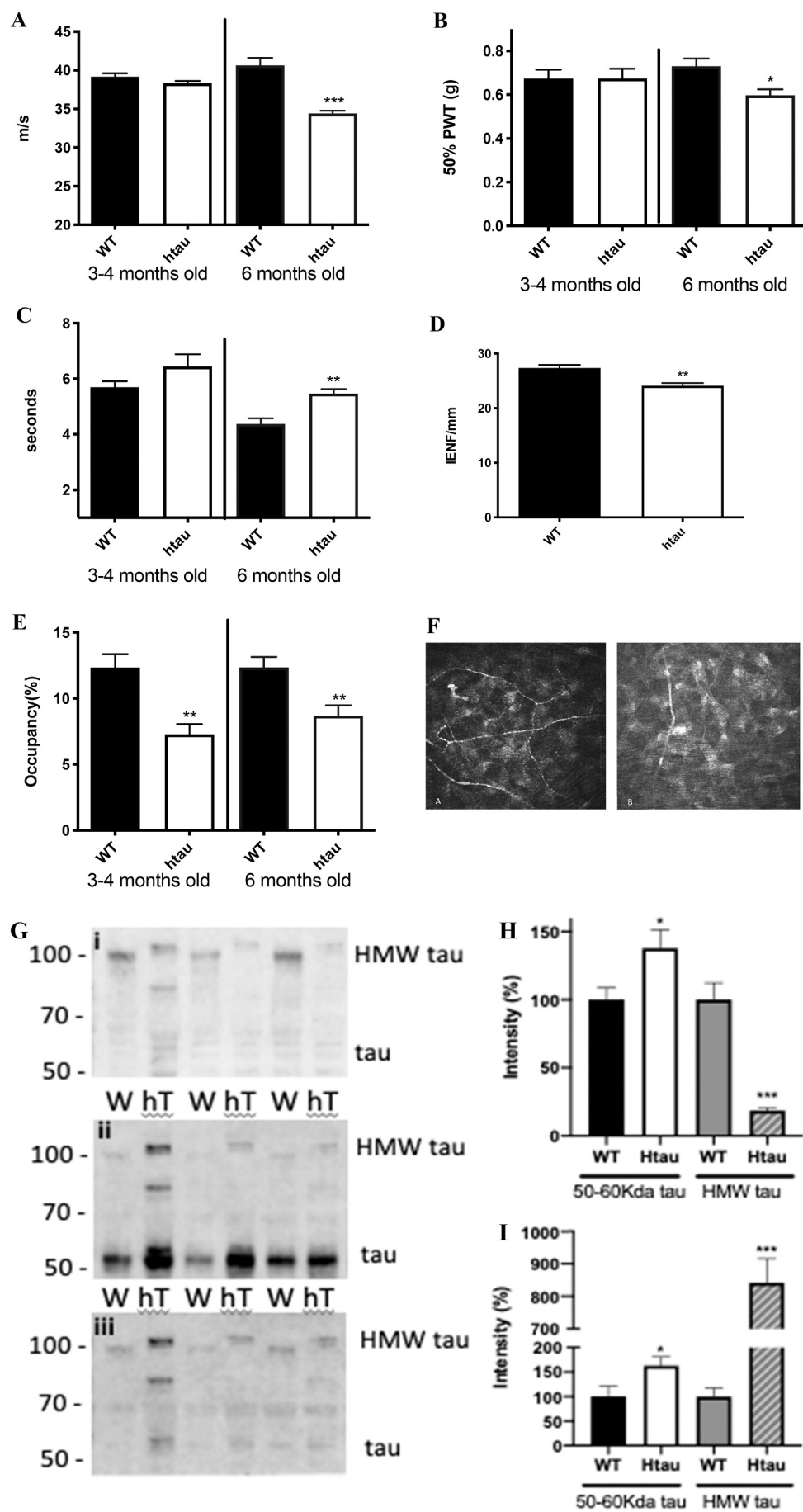
**Fig. 1.** Memory impairments: (A) Htau mice do not develop deficits in learning abilities in the Barnes maze up to 6 months of age. (B) Six months old htau mice developed 3-day memory retention deficits in the Barnes maze and (C) short-term episodic memory assessed using the Object recognition test was impaired in 6 months old htau mice.  $N = 6-10$ , \* $p < 0.05$ , \*\* $p < 0.01$  unpaired  $t$ -test versus wild type (WT) group.

diabetes along with increased phosphorylated tau levels (Jolivald et al., 2008). Here, we showed that overexpression of hyperphosphorylated human tau without an alteration in insulin signaling was sufficient to induce memory impairment by 6 months of age.

For the first time, we demonstrated that overexpression of non-mutated human tau leads to both small and large fiber neuropathy with tactile allodynia, altered thermal responses and reduced IENF and MNCV in 6 month old htau mice, similar to changes observed in diabetic mice (Jolivald et al., 2016; Anderson et al., 2014; Calcutt, 2004; Jolivald et al., 2015) and APP transgenic mice (Jolivald et al., 2012). Peripheral neuropathy results from neuronal dysfunction due in part to loss of neurotrophic support (Calcutt et al., 2008), disrupted cell signaling or structural alterations. In agreement with Trujillo-Estrada et al. (Trujillo-Estrada et al., 2019), plasma levels of glucose, insulin and insulin signaling (data not shown) were not affected by tau overexpression. Structural alterations are more likely as tau is known to play an important role in stabilizing neuronal microtubules and regulating axonal transport (Weingarten et al., 1975; 2019) and as evidenced by IENF and stromal corneal nerve loss. Htau mice expressed 2 forms of tau in the sciatic nerve, the 50–60 kDa tau and the HMW tau. As expected, 50–60 kDa tau protein levels were significantly elevated, due to human tau overexpression. In contrast, HMW tau levels were significantly reduced in htau mice, probably resulting from partial lack of mouse tau and the specific overexpression of 3R-4R human tau (Andorfer et al., 2003). Phosphorylation of tau was significantly increased for both forms of tau, the small amount of HMW being highly phosphorylated. Currently, we cannot distinguish if the phosphorylated 50–60 kDa tau, phosphorylated HMW tau or both contribute to the peripheral neuropathy observed. However, phosphorylation of tau appeared to contribute to the peripheral neuropathy in htau mice. Our results also suggest that tauopathy may be considered a systemic disorder as suggested for AD (Jolivald et al., 2012; Joachim and Selkoe, 1989).

Furthering the systemic effect of tauopathy, we have detected an early reduction of corneal nerves in htau mice. In addition to diabetic neuropathy (Malik et al., 2003; Perkins et al., 2018), a number of recent studies have reported a decrease in the sub-basal corneal nerves in patients with Parkinson's disease (Kass-Iliyya et al., 2015; De Silva et al., 2017; Podgorny et al., 2016b), multiple sclerosis (Bitirgen et al., 2017; Mikolajczak et al., 2017) and dementia (Al-Janahi et al., 2020). Recently, a study in mutated tau transgenic mice reported a decrease in sub-basal corneal nerves in 11-month old but not 6 or 8 month old mice, but did not assess stromal nerves (Jiao et al., 2020). In the present study, the most striking abnormality was a loss of stromal nerves by 3 months of age with preservation of sub-basal corneal nerves, possibly as a result of sprouting of the remaining fibers. The early and selective loss of stromal nerves in human tau mice may indicate a somatofugal neuropathy. This contrasts with diabetic neuropathy where a decrease in the sub-basal nerve plexus precedes the loss of stromal nerves, indicative of a dying back neuropathy (Chen et al., 2013). Furthermore, stromal corneal nerve loss was apparent in transgenic tau mice at 3 months of age, before an abnormality in any other indices of peripheral neuropathy or memory deficits.

The criteria for FTD subtypes are subjective and contribute to the diagnostic complexity (Landqvist Waldo et al., 2015). An objective determination of underlying neurodegeneration would benefit diagnostic and potential treatment strategies. Thus, stromal nerve analysis using the non-invasive technique of CCM may allow early detection of tau-associated neurodegeneration, especially in pre-symptomatic FTD. It could also be used in clinical trials to identify and recruit more homogeneous cohorts of patients with FTD and assess the efficacy of potential therapeutics. Additional studies are required to define the role of tau in FTD neurodegeneration and the utility of CCM as an early biomarker of FTD. However, the fact that a model of AD without overexpression of tau, did not show a decrease in stromal nerves, and that a similar AD model with tau overexpression developed stromal nerve degeneration encourages this pursuit. Our translational observations



showed a trend for reduced stromal corneal nerves in patients with FTD with preservation of sub-basal nerves, whilst there was an increase in stromal nerves with a decrease in sub-basal nerves in patients with AD. Larger studies are required to confirm if CCM could be used for the detection of neurodegeneration in early FTD and to distinguish it from other neurodegenerative diseases such as AD.

## 5. Conclusion

Overexpression of human non-mutated tau is sufficient to induce memory deficits and peripheral neuropathy in mice, suggesting that tauopathy/FTD may be a systemic disorder. Stromal corneal nerve loss precedes memory deficits in htau mice with a somatofugal pattern and preservation of more distal sub-basal nerves. This particular somatofugal degeneration detected using CCM in htau mice and FTD patients may have clinical utility as a non-invasive imaging biomarker of neurodegeneration in pre-symptomatic FTD.

## Authors contributions

Alex Marquez: Investigation, Formal analysis, Writing-Review & Editing, Lucie S Guernsey: Investigation, Katie E Frizzi: Investigation, Morgan Cundiff: Investigation Isabelle Constantino: Investigation, Nabeel Muttalib: Investigation Fernanda Arenas: Investigation, Xiajun Zhou: Investigation, Sze Hway Lim: Resources, Maryam Ferdousi: Resources, Investigation, Georgios Ponirakis: Resources, Monty Silverdale: Resources, Writing-Review & Editing Christopher Kobylecki: Resources, Matthew Jones: Resources, Andrew Marshall: Resources, Writing-Review & Editing, Rayaz A Malik: Resources, Writing-Review & Editing, Corinne G Jolival: Conceptualization, Formal Analysis, Writing-Original Draft, Supervision.

## Funding source

This work was supported by the National Institutes of Health (AG039736) to CGJ and by the Qatar Foundation (NPRP12S-0213-190080) to RAM.

Authors have no conflict of interest.

## Appendix A. Supplementary data

Supplementary data to this article can be found online at <https://doi.org/10.1016/j.nbd.2021.105273>.

**Fig. 2.** Peripheral neuropathy: Htau mice developed MNCV slowing (A), Tactile allodynia (B) and thermal hypoalgesia (C) accompanied by reduction in IENF (D) by 6 months of age. Stromal corneal nerve occupancy assessed in the stromal layer was reduced by 3 months of age (E, and stromal nerve images in F (A WT, B hTau)  $N = 7-10$ . (G) Western blot images of sciatic nerve homogenates for wild type (W) and htau (hT) mice, (i) immunoblotted for HMW tau, (ii) total tau with Tau 5 antibodies and (iii) for phosphorylated T231 tau. Note the different molecular weight of the HMW tau between wild type and htau mice. (H) Intensity of the bands corresponding to tau (around 50-60 kDa) and HMW tau, (I) Intensity of the bands corresponding to phosphorylated tau/tau (around 50-60 kDa) and phosphorylated HMW tau/HMW tau,  $N = 7$ . \* $p < 0.05$ , \*\* $p < 0.01$ , \*\*\* $p < 0.001$ , unpaired t-test versus wild type group.

## References

- Ahmed, R.M., Irish, M., van Eersel, J., et al., 2017. Mouse models of frontotemporal dementia: a comparison of phenotypes with clinical symptomatology. *Neurosci. Biobehav. Rev.* 74, 126–138.
- Takashima, A., Wolozin, B., Buee, L., 2019. Tau biology. *Adv. Exp. Med. Biol.* 1184.
- Al-Janahi, E., Ponirakis, G., Al Hamad, H., et al., 2020. Corneal nerve and brain imaging in mild cognitive impairment and dementia. *J. Alzheimers Dis.* 77, 1533–1543.
- Anderson, N.J., King, M.R., Delbruck, L., Jolival, C.G., 2014. Role of insulin signaling impairment, adiponectin and dyslipidemia in peripheral and central neuropathy in mice. *Dis. Model. Mech.* 7, 625–633.
- Andorfer, C., Kress, Y., Espinoza, M., et al., 2003. Hyperphosphorylation and aggregation of tau in mice expressing normal human tau isoforms. *J. Neurochem.* 86, 582–590.
- Bitirgen, G., Akpinar, Z., Malik, R.A., Ozkagnici, A., 2017. Use of corneal confocal microscopy to detect corneal nerve loss and increased dendritic cells in patients with multiple sclerosis. *JAMA Ophthalmol* 135, 777–782.
- Brier, M.R., Gordon, B., Friedrichsen, K., et al., 2016. Tau and Abeta imaging, CSF measures, and cognition in Alzheimer's disease. *Sci. Transl. Med.* 8, 338ra366.
- Calcutt, N.A., 2004. Experimental models of painful diabetic neuropathy. *J. Neurol. Sci.* 220, 137–139.
- Calcutt, N.A., Jolival, C.G., Fernyhough, P., 2008. Growth factors as therapeutics for diabetic neuropathy. *Curr. Drug Targets* 9, 47–59.
- Chen, D.K., Frizzi, K.E., Guernsey, L.S., Lad, K., Mizisin, A.P., Calcutt, N.A., 2013. Repeated monitoring of corneal nerves by confocal microscopy as an index of peripheral neuropathy in type-1 diabetic rodents and the effects of topical insulin. *J. Peripher. Nerv. Syst.* 18, 306–315.
- Dabbah, M.A., Graham, J., Petropoulos, I.N., Tavakoli, M., Malik, R.A., 2011. Automatic analysis of diabetic peripheral neuropathy using multi-scale quantitative morphology of nerve fibres in corneal confocal microscopy imaging. *Med. Image Anal.* 15, 738–747.
- De Silva, M.E.H., Zhang, A.C., Karahalios, A., Chinnery, H.R., Downie, L.E., 2017. Laser scanning in vivo confocal microscopy (IVCM) for evaluating human corneal sub-basal nerve plexus parameters: protocol for a systematic review. *BMJ Open* 7, e018646.
- Ennaceur, A., Delacour, J., 1988. A new one-trial test for neurobiological studies of memory in rats. 1: Behavioral data. *Behav. Brain Res.* 31, 47–59.
- Goedert, M., Eisenberg, D.S., Crowther, R.A., 2017. Propagation of tau aggregates and neurodegeneration. *Annu. Rev. Neurosci.* 40, 189–210.
- Hanger, D.P., Goniotaki, D., Noble, W., 2019. Synaptic localisation of tau. *Adv. Exp. Med. Biol.* 1184, 105–112.
- Hornberger, M., Piguet, O., 2012. Episodic memory in frontotemporal dementia: a critical review. *Brain* 135, 678–692.
- Hornberger, M., Piguet, O., Graham, A.J., Nestor, P.J., Hodges, J.R., 2010. How preserved is episodic memory in behavioral variant frontotemporal dementia? *Neurology* 74, 472–479.
- Hutton, M., Lendon, C.L., Rizzu, P., et al., 1998. Association of missense and 5'-splice-site mutations in tau with the inherited dementia FTDP-17. *Nature* 393, 702–705.
- Irish, M., Piguet, O., Hodges, J.R., Hornberger, M., 2014. Common and unique gray matter correlates of episodic memory dysfunction in frontotemporal dementia and Alzheimer's disease. *Hum. Brain Mapp.* 35, 1422–1435.
- Jiao, H., Downie, L.E., Huang, X., et al., 2020. Novel alterations in corneal neuroimmune phenotypes in mice with central nervous system tauopathy. *J. Neuroinflammation* 17, 136.
- Joachim, C.L., Selkoe, D.J., 1989. Amyloid protein in Alzheimer's disease. *J. Gerontol.* 44, B77–B82.
- Johnson, K.A., Schultz, A., Betensky, R.A., et al., 2016. Tau positron emission tomographic imaging in aging and early Alzheimer disease. *Ann. Neurol.* 79, 110–119.

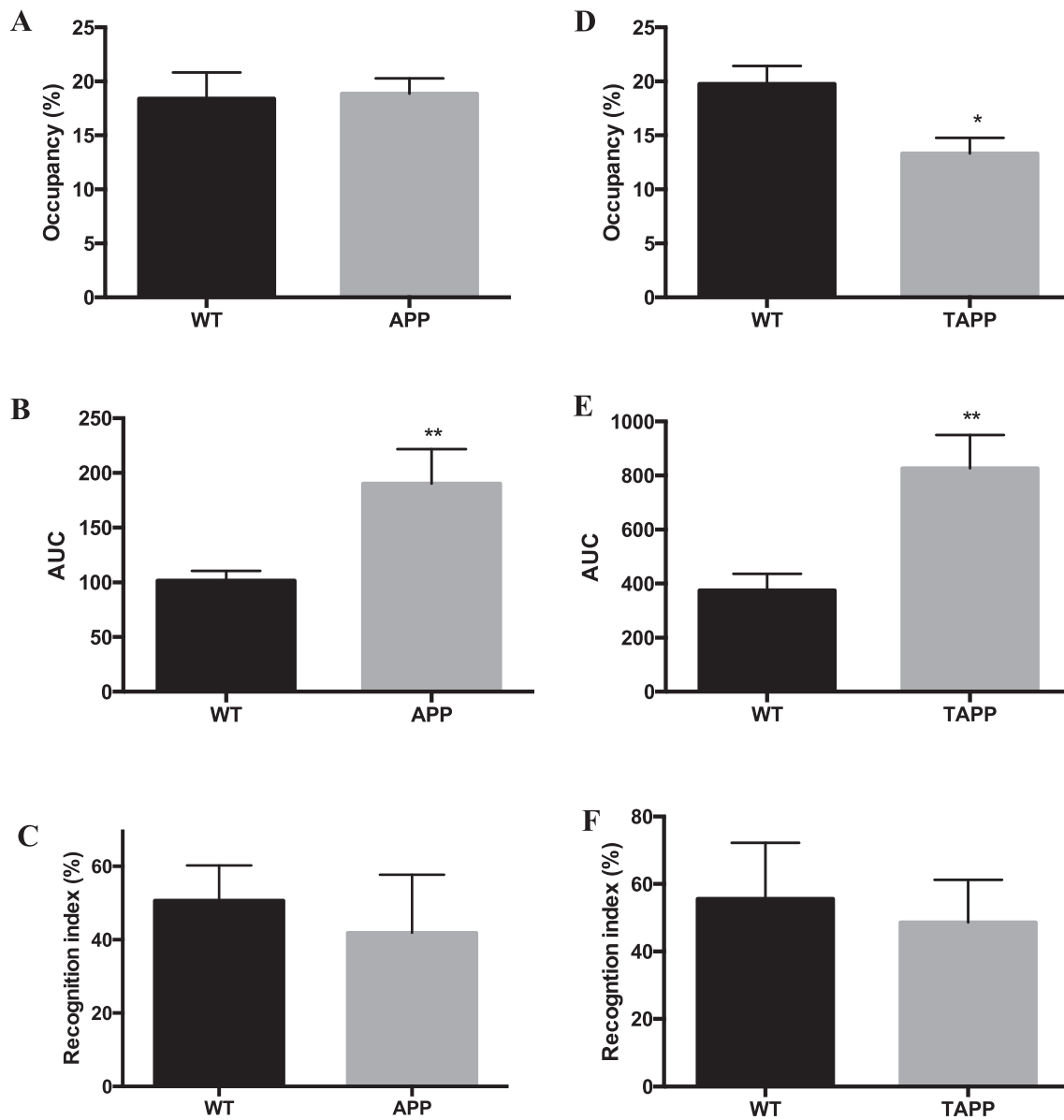


**Fig. 3.** APP and TAPP mice: Stromal corneal nerve occupancy (A), Area under the curve for the acquisition phase of the Barnes maze (B) and Recognition index in the object recognition test (C) for 1 year old APP mice, ( $N = 5-8$ ). Stromal corneal nerve occupancy (D), Area under the curve for the acquisition phase of the Barnes maze (E) and Recognition index in the object recognition test (F) for 4-month old TAPP mice,  $N = 8-10$ . \* $p < 0.05$ , \*\* $p < 0.01$ , unpaired  $t$ -test versus Wild type (WT) group.

**Table 2**

Demographic characteristics and corneal nerve occupancy of FTD and AD subjects.

	Control ( $N = 3$ )	FTD ( $N = 2$ )	Control ( $N = 6$ )	AD ( $N = 3$ )
Age, years	$57.6 \pm 11.9$	$61.5 \pm 13.4$	$77.3 \pm 5.3$	$77.1 \pm 5.0$
Sex (Male, Female)	(3,0)	(2,0)	(3,3)	(2,1)
MoCA	nd	28.0	$27.3 \pm 3.2$	$11.3 \pm 9.8$
Corneal nerve occupancy (pixels)	$59.7 \pm 12.3$	$36.0 \pm 8.4$	$65.0 \pm 45.3$	$180.7 \pm 66.9$

Jolival, C.G., Lee, C.A., Beiswenger, K.K., et al., 2008. Defective insulin signaling pathway and increased glycogen synthase kinase-3 activity in the brain of diabetic mice: parallels with Alzheimer's disease and correction by insulin. *J. Neurosci. Res.* 86, 3265–3274.

- Jolival, C.G., Hurford, R., Lee, C.A., Dumaop, W., Rockenstein, E., Masliah, E., 2010. Type 1 diabetes exaggerates features of Alzheimer's disease in APP transgenic mice. *Exp. Neurol.* 223, 422–431.
- Jolival, C.G., Calcott, N.A., Masliah, E., 2012. Similar pattern of peripheral neuropathy in mouse models of type 1 diabetes and Alzheimer's disease. *Neuroscience* 202, 405–412.
- Jolival, C.G., Rodriguez, M., Wahren, J., Calcott, N.A., 2015. Efficacy of a long-acting C-peptide analogue against peripheral neuropathy in streptozotocin-diabetic mice. *Diabetes Obes. Metab.* 17, 781–788.
- Jolival, C.G., Frizzi, K.E., Guernsey, L., et al., 2016. Peripheral neuropathy in mouse models of diabetes. *Curr. Protoc. Mouse Biol.* 6, 223–255.
- Kalteniece, A., Ferdousi, M., Adam, S., et al., 2017. Corneal confocal microscopy is a rapid reproducible ophthalmic technique for quantifying corneal nerve abnormalities. *PLoS One* 12, e0183040.
- Kass-Ilyya, L., Javed, S., Gosal, D., et al., 2015. Small fiber neuropathy in Parkinson's disease: a clinical, pathological and corneal confocal microscopy study. *Parkinsonism Relat. Disord.* 21, 1454–1460.
- King, M.R., Anderson, N.J., Deciu, M., et al., 2020. Insulin deficiency, but not resistance, exaggerates cognitive deficits in transgenic mice expressing human amyloid and tau proteins. Reversal by Exendin-4 treatment. *J. Neurosci. Res.* 98, 2357–2369.
- Landqvist Waldo, M., Gustafson, L., Passant, U., Englund, E., 2015. Psychotic symptoms in frontotemporal dementia: a diagnostic dilemma? *Int. Psychogeriatr.* 27, 531–539.

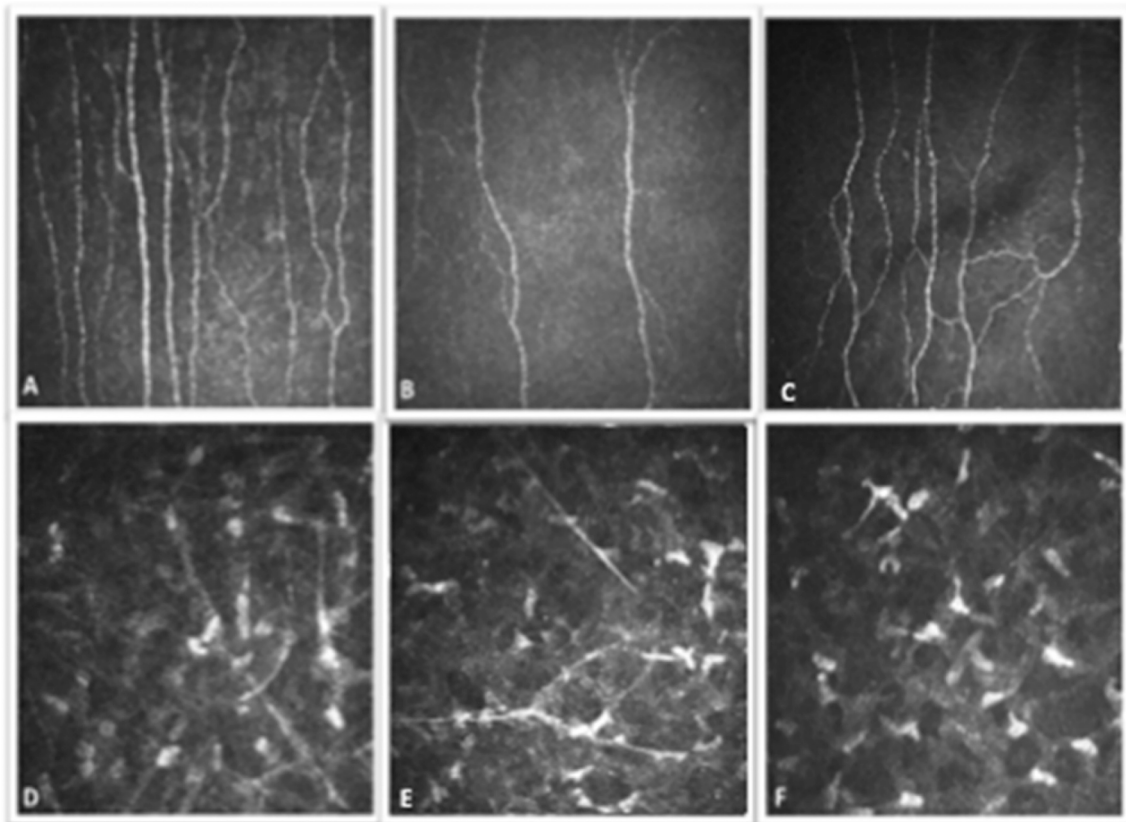


**Fig. 4.** Corneal nerves in FTD and AD patients. Corneal nerve images (Top row: sub-basal Bowman's layer, Bottom row: Stromal layer, A, D: control, B, E: Alzheimer's disease patient, C, F: Frontotemporal dementia patient).

- Lewis, J., Dickson, D.W., Lin, W.L., et al., 2001. Enhanced neurofibrillary degeneration in transgenic mice expressing mutant tau and APP. *Science* 293, 1487–1491.
- Lowe, V.J., Wiste, H.J., Senjem, M.L., et al., 2018. Widespread brain tau and its association with ageing, Braak stage and Alzheimer's dementia. *Brain* 141, 271–287.
- Malik, R.A., Kallinikos, P., Abbott, C.A., et al., 2003. Corneal confocal microscopy: a non-invasive surrogate of nerve fibre damage and repair in diabetic patients. *Diabetologia* 46, 683–688.
- Mikolajczak, J., Zimmermann, H., Kheirikhah, A., et al., 2017. Patients with multiple sclerosis demonstrate reduced subbasal corneal nerve fibre density. *Mult. Scler.* 23, 1847–1853.
- Orr, M.E., Sullivan, A.C., Frost, B., 2017. A brief overview of Tauopathy: causes, consequences, and therapeutic strategies. *Trends Pharmacol. Sci.* 38, 637–648.
- Pennington, C., Hodges, J.R., Hornberger, M., 2011. Neural correlates of episodic memory in behavioral variant frontotemporal dementia. *J. Alzheimers Dis.* 24, 261–268.
- Perkins, B.A., Lovblom, L.E., Bril, V., et al., 2018. Corneal confocal microscopy for identification of diabetic sensorimotor polyneuropathy: a pooled multinational consortium study. *Diabetologia* 61, 1856–1861.
- Phillips, M., Boman, E., Osterman, H., Willhite, D., Laska, M., 2011. Olfactory and visuospatial learning and memory performance in two strains of Alzheimer's disease model mice—a longitudinal study. *PLoS One* 6, e19567.
- Podgorny, P.J., Suchowersky, O., Romanchuk, K.G., Feasby, T.E., 2016a. Evidence for small fiber neuropathy in early Parkinson's disease. *Parkinsonism Relat. Disord.* 28, 94–99.
- Podgorny, P.J., Pratt, L.M., Liu, Y., et al., 2016b. Low counts of B cells, natural killer cells, monocytes, dendritic cells, basophils, and eosinophils are associated with postengraftment infections after allogeneic hematopoietic cell transplantation. *Biol Blood Marrow Transplant* 22, 37–46.
- Polydoro, M., Acker, C.M., Duff, K., Castillo, P.E., Davies, P., 2009. Age-dependent impairment of cognitive and synaptic function in the htau mouse model of tau pathology. *J. Neurosci.* 29, 10741–10749.
- Ponirakis, G., Al Hamad, H., Sankaranarayanan, A., et al., 2019. Association of corneal nerve fiber measures with cognitive function in dementia. *Ann Clin Transl Neurol* 6, 689–697.
- Poorakaj, P., Bird, T.D., Wijsman, E., et al., 1998. Tau is a candidate gene for chromosome 17 frontotemporal dementia. *Ann. Neurol.* 43, 815–825.
- Ramsden, M., Kotilinek, L., Forster, C., et al., 2005. Age-dependent neurofibrillary tangle formation, neuron loss, and memory impairment in a mouse model of human tauopathy (P301L). *J. Neurosci.* 25, 10637–10647.
- Regan, P., Whitcomb, D.J., Cho, K., 2017. Physiological and pathophysiological implications of synaptic tau. *Neuroscientist* 23, 137–151.
- Roberson, E.D., 2012. Mouse models of frontotemporal dementia. *Ann. Neurol.* 72, 837–849.
- Rockenstein, E., Mallory, M., Mante, M., Sisk, A., Masliah, E., 2001. Early formation of mature amyloid-beta protein deposits in a mutant APP transgenic model depends on levels of Abeta(1-42). *J. Neurosci. Res.* 66, 573–582.
- Rockenstein, E., Adame, A., Mante, M., Moessler, H., Windisch, M., Masliah, E., 2003. The neuroprotective effects of Cerebrolysin in a transgenic model of Alzheimer's disease are associated with improved behavioral performance. *J. Neural Transm. (Vienna)* 110, 1313–1327.
- Rockenstein, E., Mante, M., Adame, A., Crews, L., Moessler, H., Masliah, E., 2007. Effects of Cerebrolysin on neurogenesis in an APP transgenic model of Alzheimer's disease. *Acta Neuropathol.* 113, 265–275.
- Santacruz, K., Lewis, J., Spire, T., et al., 2005. Tau suppression in a neurodegenerative mouse model improves memory function. *Science* 309, 476–481.
- Spillantini, M.G., Crowther, R.A., Goedert, M., 1996. Comparison of the neurofibrillary pathology in Alzheimer's disease and familial presenile dementia with tangles. *Acta Neuropathol.* 92, 42–48.
- Tatebayashi, Y., Miyasaka, T., Chui, D.H., et al., 2002. Tau filament formation and associative memory deficit in aged mice expressing mutant (R406W) human tau. *Proc. Natl. Acad. Sci. U. S. A.* 99, 13896–13901.
- Tolkovsky, A.M., Brelstaff, J., 2018. Sensory neurons from tau transgenic mice and their utility in drug screening. *Methods Mol. Biol.* 1727, 93–105.
- Trujillo-Estrada, L., Nguyen, C., da Cunha, C., et al., 2019. Tau underlies synaptic and cognitive deficits for type 1, but not type 2 diabetes mouse models. *Aging Cell* 18, e12919.
- Vacchi, E., Kaelin-Lang, A., Melli, G., 2020. Tau and alpha Synuclein synergistic effect in neurodegenerative diseases: when the periphery is the Core. *Int. J. Mol. Sci.* 21.
- Weingarten, M.D., Lockwood, A.H., Hwo, S.Y., Kirschner, M.W., 1975. A protein factor essential for microtubule assembly. *Proc. Natl. Acad. Sci. U. S. A.* 72, 1858–1862.
- Yi, S., Liu, Q., Wang, X., et al., 2019. Tau modulates Schwann cell proliferation, migration and differentiation following peripheral nerve injury. *J. Cell Sci.* 132.